Optical design and development of a fiber coupled high-power diode laser system for laser transmission welding of plastics

Eva Rodríguez-Vidal
Iban Quintana
Jon Etxarri
Urko Azkorbebeitia
Deitze Otaduy
IK4-TEKNIKER
Polo Tecnológico de Eibar
Calle Iñaki Goenaga, 5
20600 Eibar, Gipuzkoa, Spain
E-mail: erodriguez@tekniker.es

Francisco González
Fernando Moreno
University of Cantabria
Group of Optics
Applied Physics Department
Avenida de los Castros, s/n
39005, Santander, Spain

Abstract. Laser transmission welding (LTW) of thermoplastics is a direct bonding technique already used in different industrial applications sectors such as automobiles, microfluidics, electronics, and biomedicine. LTW evolves localized heating at the interface of two pieces of plastic to be joined. One of the plastic pieces needs to be optically transparent to the laser radiation whereas the other part has to be absorbent, being that the radiation produced by high power diode lasers is a good alternative for this process. As consequence, a tailored laser system has been designed and developed to obtain high quality weld seams with weld widths between 0.7 and 1.4 mm. The developed laser system consists of two diode laser bars (50 W per bar) coupled into an optical fiber using a nonimaging solution: equalization of the beam parameter product (BPP) in the slow and fast axes by a pair of step-mirrors. The power scaling was carried out by means of a multiplexing polarization technique. The analysis of energy balance and beam quality was performed considering ray tracing simulation (ZEMAX®) and experimental validation. The welding experiments were conducted on acrylonitrile/butadiene/styrene (ABS), a thermoplastic frequently used in automotive, electronics and aircraft applications, doped with two different concentrations of carbon nanotubes (0.01% and 0.05% CNTs). Quality of the weld seams on ABS was analyzed in terms of the process parameters (welding speed, laser power and clamping pressure) by visual and optical microscope inspections. Mechanical properties of weld seams were analyzed by mechanical shear tests. High quality weld seams were produced in ABS, revealing the potential of the laser developed in this work for a wide range of plastic welding applications.
[DOI: 10.1117/1.OE.51.12.124301]

Subject terms: laser transmission welding; polymer; carbon nanotubes; high power diode laser bars; beam quality; optical design; polarization multiplexing.

Paper 121038P received Jul. 17, 2012; revised manuscript received Oct. 22, 2012; accepted for publication Nov. 7, 2012; published online Dec. 5, 2012.

1 Introduction

Over the past few years, plastic welding techniques have attracted a considerable interest from several industrial sectors such as automotive, packaging and healthcare.[1–5] Depending on the application and technical requirements of the component, joining of thermoplastics can be divided into mechanical fastening, adhesive and fusion bonding.[1,6,7] Laser transmission welding (LTW) belongs to the last category and it is usually used in applications where the hermetic adhesion and the minimization of the surrounding affected area are critical requirements.[5,7,8–11] LTW involves localized heating at the interface of two pieces of plastic to be joined. Therefore, one of the plastics needs to be optically transparent to the laser radiation whereas the other one has to be absorbent. The laser energy that is absorbed in this material causes vibration of electron bonds, followed by heat transfer to the surroundings through convection and radiation. When heated to temperatures above the melting point (or glass transition temperature in the case of amorphous thermoplastics), the material begins to flow and a weld is formed while applying a pressure to increase mating contact forces. The molten plastic improves the heat contact between both parts and involves an internal joining pressure to build up through volume expansion. Depending on the optical and thermal properties of the absorbent part, the incident radiation is absorbed over a certain depth of the absorbent material.[12–14]

In the case of CO_2 laser systems ($\lambda = 10.6$ μm), the beam is rapidly absorbed in the upper layers of the material when a laser radiation is applied to a plastic. It is a consequence of the high absorption coefficient of thermoplastic to medium infrared radiation. For this reason, CO_2 laser systems have been traditionally used in welding application of thin plastic films but not in welding thicker sheets. By contrast, the radiation produced by high power diode lasers ($\lambda = 808$ nm, 908 nm), is less readily absorbed by plastics and, together with the fact that these systems show high electro-optical efficiency, make them a very good alternative for LTW of thermoplastics.[7,14–16] They can be applied to a given material either directly from the diode laser bars or by means of a fiber optics arrangement.[16] In this case, the laser-fiber coupling is not straightforward since the radiation emitted

0091-3286/2012/$25.00

from high power diode lasers (HPDL) bars suffers from two asymmetries: astigmatism and elliptical beam profile. Thus, the divergence angles are different in the two axes, so-called "fast-axis" and "slow-axis". The emerging laser beam is a stripe with different beam profiles in both directions.[17–19] Different approaches have been proposed for diode laser beam shaping to obtain a circular focus spot. Zbinden et al. and Graf et al.[20,21] considered a diode laser bar coupled into a multitude of fibers leading to a fiber bundle at the output end. Yamaguchi et al.[22] studied a multiprism array leading to a short dotted lines arrangement in parallel direction. Clarkson et al.[23] proposed two plane parallel mirrors to reshape the diode laser bars emission. Ehlers et al. and Treush et al.[18,24] employed step-mirrors to rearrange the emission from the diode laser bars and to couple it into an optical fiber. This method is currently a well-known and efficient technique with easy alignment requirements and low manufacturing costs.

To increase the output power compared with a single diode laser bar, the emission of multiple diode laser bars has to be combined. In this way, incoherent beam combination of individual diode laser bars has been frequently used in laser systems for material processing. The basic techniques used to increase output power at constant beam size are called wavelength and polarization multiplexing.[18,25]

The objective of the present work is to build a tailored diode laser system for a specific laser material processing application: welding of thermoplastic using the LTW technique. The welding application described in this work is focused on assembly of miniaturized components (plastic devices). Therefore, a laser spot with specific requirements regarding size, quality and output power (up to 50 W) are needed in order to carry out the welding process in a productive way. The fact of designing and developing the fiber-coupled high-power diode laser system instead of using a commercial diode laser system provides a meaningful versatility to customize it depending on the requirement of the laser application. In this sense, small modifications to the developed laser system, such as optical output power wavelength and diameter optical fiber, could be performed to be used for other laser material processing applications.

With this aim, a previous modeling of the laser system based on ZEMAX ray-tracing software is reported. Comparison of modeling calculations with experimental results in terms of beam quality in different stages of the optical design is performed. The system consists of a pair of step-mirrors for beam shaping. The modular design permits power scaling using the polarization multiplexing technique. The beam quality factor is analyzed to guarantee a high coupling efficiency to a selected optical fiber ($\Phi = 600/400\ \mu$m, NA = 0.22). More specifically, the diode laser system is employed for LTW of acrylonitrile/butadiene/styrene (ABS), a thermoplastic frequently used in the automotive sector. The quality of the weld seams on ABS is analyzed in terms of its optical properties by changing the material microstructure.

The paper is organized as follows. Section 2 describes the optical design of the laser system based on the use of two micro step-mirror and multiplexing polarization technique, modeled using the ZEMAX® ray tracing software. Section 3 concerns experimental characterization of the laser system prototype by means of polarization and beam shaping analysis. Section 4 presents LTW experiments on ABS plates by means of the laser developed in this work. The quality of the weld seams is analyzed in terms of the process parameters by means of visual optical microscope inspection and the mechanical shear tests. Finally, the main conclusions are presented in Sec. 5.

2 Optical System Design

The diode laser bars are linear arrangement of large area emitters of incoherent radiation characterized by astigmatism and elliptical beam profile. In this paper, double sided micro-optical arrays are used for fast axis (FAC) and slow axis (SAC) collimation, reducing the asymmetric divergence and improving the beam quality.[25] The laser sources considered are two similar diode laser bars from Jenoptik Laser GmbH (JOLD-50-CPBN-1L).[26] Each bar consists of 19 broad area emitters (collimation in both axes (FAC < 0.5- deg, SAC < 4- deg) and 30% Fill Factor) with a maximum output power per bar of about 50 W CW at $\lambda = 808 \pm 4$ nm.

The beam quality of a diode laser bar is usually quantified by the BPP* defined as a product of the beam waist and the beam divergence at half angle in the far field. The BPP corresponding to the slow axis direction depends on the number of emitters and the fill factor.[27,28] The BPP of the laser beam in the diagonal direction (BPP_{total}) is calculated from the BPP of the laser beam in the slow and fast axis (BPP_{slow} and BPP_{fast}). A simple geometrical consideration shows that efficient fiber coupling of a diode laser beam requires a BPP_{total} given[29] by the Eq. (1):

$$BPP_{total} = \sqrt{BPP_{slow}{}^2 + BPP_{fast}{}^2} \leq BPP_{fiber} = \frac{d_{fiber}}{2} \times NA, \tag{1}$$

where BPP_{fiber}, d_{fiber} and NA denote the BPP, diameter and numerical aperture of the optical fiber, respectively.

Due to the highly asymmetric output beam profile from the diode laser bar, efficient fiber coupling is only possible if the different BPPs are adapted by shifting beam quality from one direction to the other direction. The symmetrization of the BPPs is equivalent to a minimization of the overall beam parameter product BPP_{total} as can be seen in Eq. (1).[28–32] Guaranteeing an efficient fiber coupling: $BPP_{total} < BPP_{fiber}$, is only possible if the symmetrization of BPPs in both axes is achieved.

The beam shaping of a JOLD-50-CPBN-1L and the coupling of the output beam into a fiber are simulated using ZEMAX® ray tracing software that operates in a non-sequential mode. The nonimaging solution is based on the symmetrization of the diode laser radiation by means of two identical step-mirrors. Each single mirror surface of the first step-mirror is tilted 45-deg. about the slow axis and separated from the neighboring surface by a constant distance d along the axis of propagation [Fig. 1(a)]. The laser beam is incident on the first step-mirror. Here, it is cut into 13 sub-beams along the slow axis direction. Each sub-beam is reflected along the fast axis direction towards the second step-mirror, leading to sub-beams reflection into the slow-direction. In order to decrease the spot size on the fast axis, an anamorphic prism pair is used, which spatially compresses the spot

*Defined as $BPP = \omega_0 \cdot \theta/2$ (half beam waist diameter w_0 times half far field divergence angle $\theta/2$).

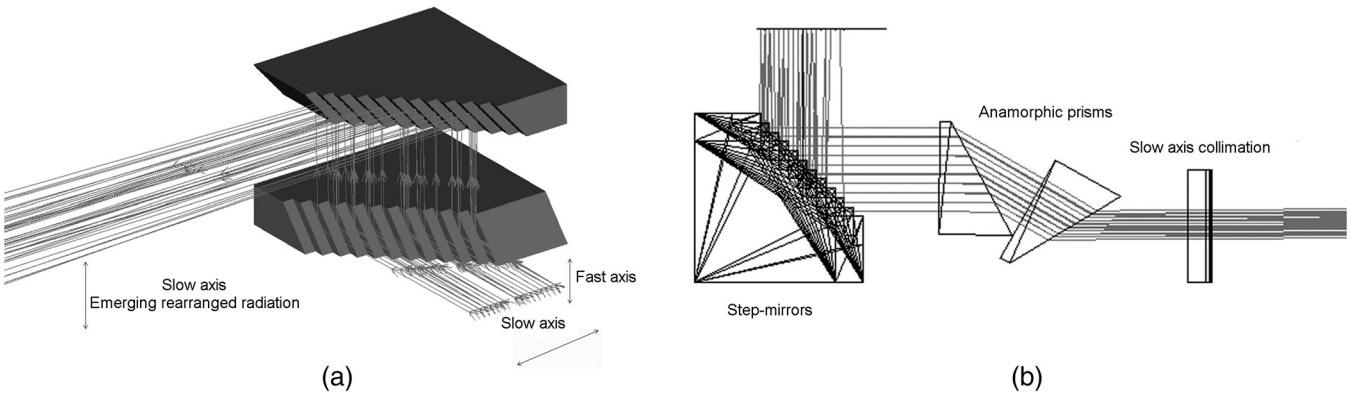

Fig. 1 (a) Realization of beam rearranging by a pair of step-mirrors consisting of 13 steps. (b) Top side view of the compression unit.

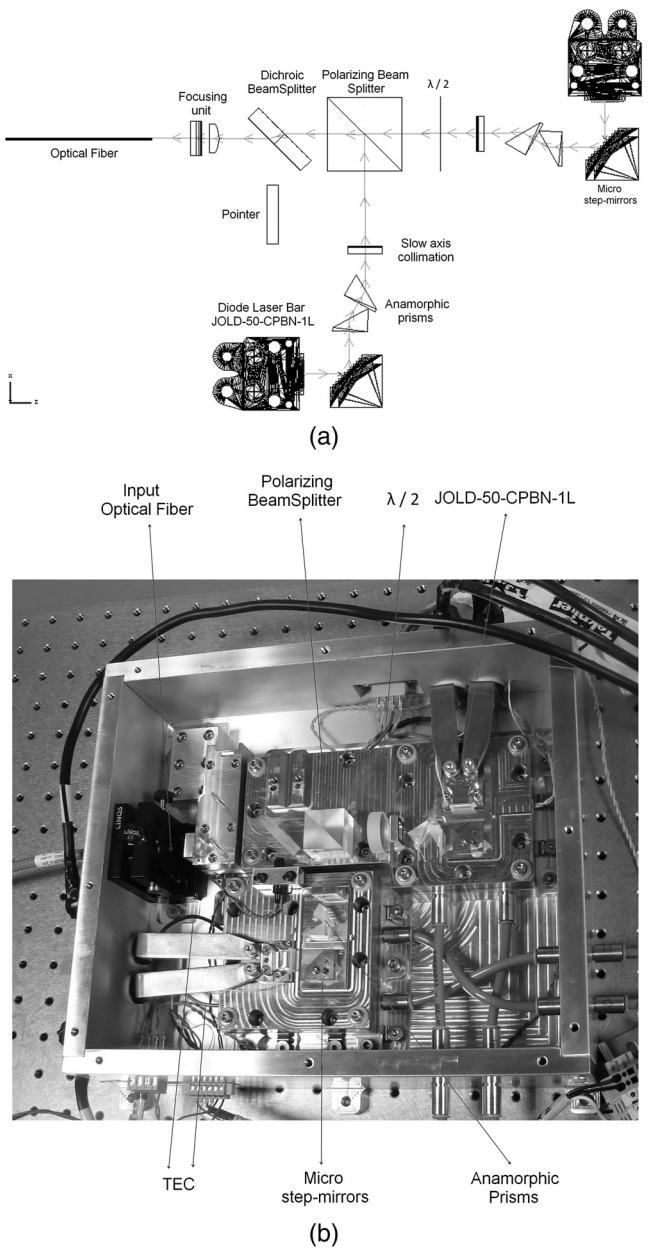

Fig. 2 (a) Optical system scheme and (b) diode laser system prototype.

height to 1/3 of its initial value. After that, a cylindrical lens is used in order to reduce the residual divergence in the slow axis [Fig. 1(b)]. The BPP resulting from this beam shaping technique along the slow axis is 21.3 mm.mrad whereas along the fast axis is 8.5 mm.mrad.

As was mentioned before, to increase the output power of the system with a single diode bar, the emission of two diode laser bars were combined by using the polarization multiplexing technique. This way, the power of the system can be increased to twice of the original, whereas the beam quality would not be influenced. As will be described in Sec. 3.1, the degree of polarization in transmission [DoP (TE)] of the radiation coming from the diode laser bars is 97%. The vibration direction of the electric field is parallel to the slow axis. Therefore, the polarization rotation of the light coming from one bar using a $\lambda/2$ wave-plate is required to allow the overlapping of the emission from the two diode bars. This overlapping has been achieved by a polarization beam splitter (PBS) [Fig. 2(a)].

Figure 2(a) represents the optical system scheme and Fig. 2(b) shows the experimental arrangement of the laser system prototype, including the cooling system performed by Peltier cooling modules (TEC) [Fig. 2(b)]. The corresponding results obtained from optical simulation and experimental development are analyzed and discussed in the next section.

3 Characterization of the Laser System Prototype

The validation of the above optical model carried out by ZEMAX® is presented in this section. The degree of polarization of the diode laser bars is performed in order to guarantee an efficient polarization multiplexing. Furthermore, the results concerning beam shaping and beam quality will be analyzed along with the fiber coupling efficiencies.

3.1 *Polarization Analysis*

The diode laser bars (JOLD-50-CPBN-1L) are TE-polarized, i.e., the main component of the electric field vector vibrates along the slow axis direction. The degree of polarization (DoP) is measured in order to predict the power losses associated with the polarizing components used in the optical system. The DoP in transmission is a measure of the randomness of polarization in a light beam[32] and can be described by the following equation:

$$\mathrm{DoP(TE)} = \frac{\bar{I}_x - \bar{I}_z}{\bar{I}_x + \bar{I}_z}, \tag{2}$$

where $\bar{I}_x$ represents the laser beam intensity measured in the plane of the junction (TE) and corresponds to the average value of the two intensities measured at polarization angles of 0-deg. and 180-deg. $\bar{I}_z$, the intensity measured in the perpendicular plane and corresponds to the average value of the two intensities measured at polarization angles of 90-deg. and 270-deg [Fig. 3(a)]. Hence, a DoP of −1 means 100% TM polarization while a DoP of 1.0 means 100% TE polarization. A DoP of 0 indicates either equal components of each polarization are present or complete random polarization.[33,34] The DoP analysis was carried out by considering a rotating Glan-Laser Calcite Polarizer (GL10-B, Thorlabs) located between the one of the diode laser bar and the thermopile. The polarization of the bar was measured every 10 deg until 360-deg. Figure 3(b) shows the system polarization graphed on a polar plot, indicating that the diode laser bar is primarily TE polarized with a DoP = 0.97. This chart reveals that, when coupling the two diode laser bars by considering a proper beam alignment, about 3% of the laser power will be lost through the PBS.

3.2 *Beam Shaping and Fiber Coupling*

Considering the emission properties of the JOLD-50-CPBN-1L behind the collimation microoptics, the asymmetric radiation provides a $\mathrm{BPP_{slow}} \sim 174$ mm.mrad and $\mathrm{BPP_{fast}} \sim 0.002$ mm.mrad. As it was stressed earlier, laser beam shaping is needed to guarantee an efficient fiber coupling ($\mathrm{BPP_{laser\text{-}beam}} < \mathrm{BPP_{fiber}}$). Experiments were performed using 600 μm and 400 μm fibers. The numerical aperture of both fibers is 0.22. According to Eq. (1), their BPP are 66.5 and 48.8 mm.mrad, respectively.

Once the beam has been shaped, i.e., the BPP has been equalized, the intensity distribution of the two laser beams has been analyzed by the ZEMAX® model, as well as experimentally (Fig. 4). Figure 4(a) shows the intensity distribution of the two laser beams emerging from the step-mirrors [Fig. 1(a)] obtained by the ZEMAX® model, and Fig. 4(b) the corresponding experimental far-field measurement (Primes Beam Monitor BM60 4623). As can be seen, the intensity distribution emerging from each step-mirror systems consists of ten stripes coming from the reflection from the individual steps of the mirror pair.[18,24] Their intensity distribution broadens from left to right side. This effect can be caused by the staircase-like displacement of each micro-mirror along the axis of propagation. Furthermore, the far left and the right stripes of each laser beam exhibit a cut-off that can be originated from the fact that the outer mirrors are not illuminated by the full slow-axis angle of the light cone of the diode laser.[24]

Figure 5 shows the simulated and measured intensity distribution of the far field laser beam behind the last stage of rearrangement: steps-mirrors + anamorphic prism pair + slow axis collimation lens [Fig. 1(b)]. It can be observed that the cross sections of the laser beams have similar dimensions in fast and slow axis, which means that a symmetrization of the laser beam has been achieved. In both cases, Figs. 4 and 5, the experimental results were well-reproduced by the ZEMAX® model. The slight deviations observed in a qualitative comparative analysis may be due to different relevant reasons in the ZEMAX® model:

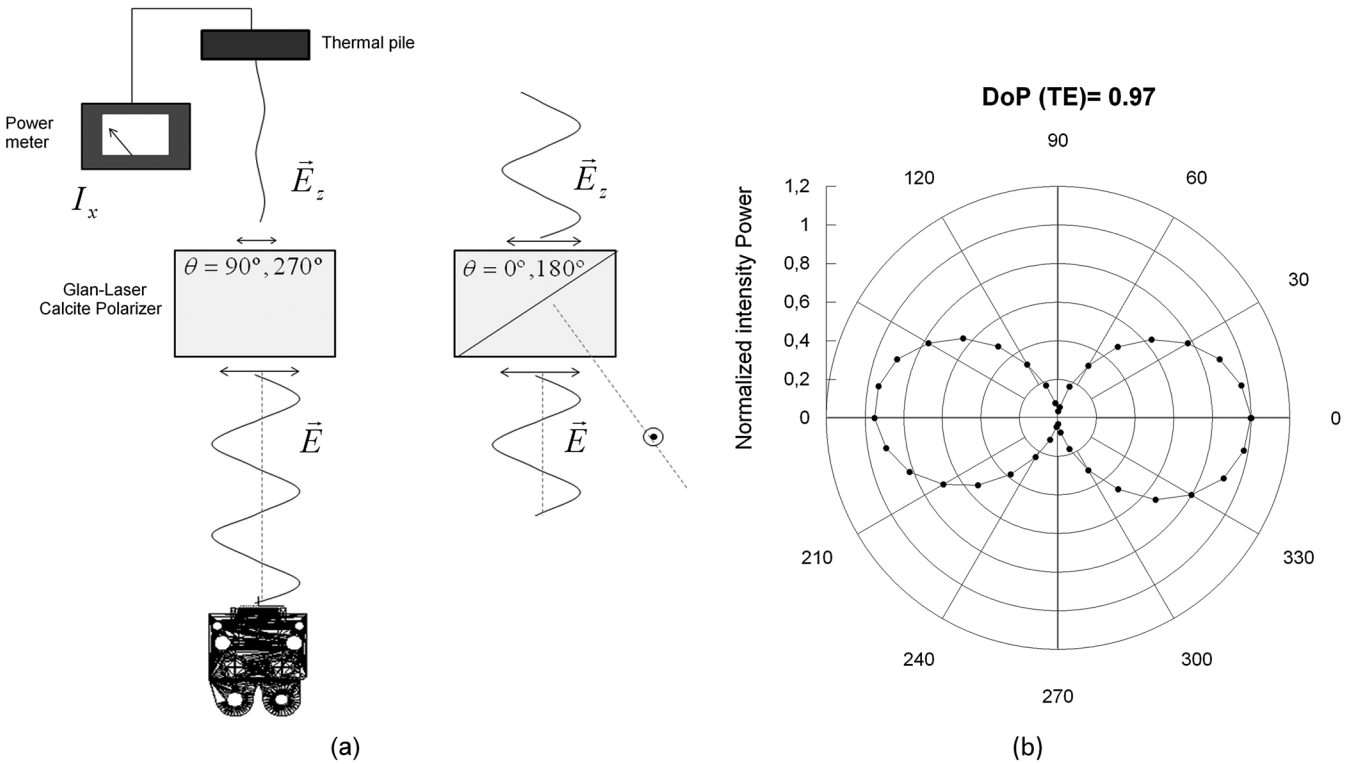

Fig. 3 (a) Schematic set-up for DoP measurement, left $\theta = 90$ deg and 270 deg, right $\theta = 0$ deg and 180 deg; and (b) polarization plot of a JOLD-50-CPBN-1L at 5 W of laser power emission.

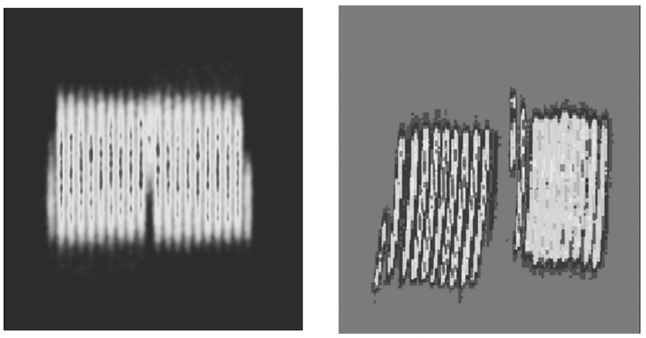

(a) (b)

Fig. 4 (a) Simulated and (b) experimental far field irradiance of the reshape laser beam after the step-mirrors at 10W of laser power emission. Vertical: slow axis, horizontal: fast axis. The detector is 30×30 mm^2.

(1) It has been assumed an equal intensity distribution for every diode laser emitter of the diode bar for near and far field distribution. This assumption is not strictly true since the laser beam power at the corners is lower than that at the center.[30]

(2) The intensity distribution simulation of each diode laser can be improved by calibrating the spatial super-Gaussian factor of the diode laser emitters.[35]

(3) It has not been taken into account possible effects of smile. This effect occurs if some emitting facets of the diode laser bar are displaced by a small distance of only μm from a straight line along the slow axis. If smile effect occurs, due to the short focal length of the diode bar micro-lens this would have a significant effect on the divergence angle after them.[24,25]

Therefore, by means of the considered beam-shaping technique it has been possible to reshape the rectangular output beam from a diode laser bar into a square laser beam with similar beam quality in both axes lower than the selected fiber BPP (Fig. 5). Both reshaped laser beams are combined by polarization multiplexing technique.

Finally, the reshaped laser beam is focused and coupled to the optical fiber, achieving a high quality and high efficiency fiber coupled diode laser system. The focusing of the slow and fast directions of the collimated laser beam has been performed by means of two cylindrical lenses (Fig. 2), with

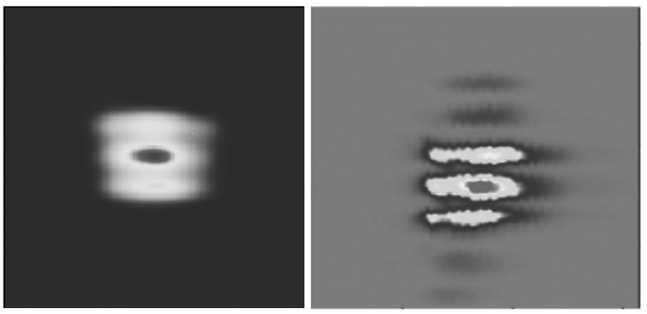

(a) (b)

Fig. 5 (a) Simulated and (b) experimental irradiance of the collimated laser beam at 10 W of laser power emission. Vertical: slow axis, horizontal: fast axis. Detector 15×15 mm^2.

focal lengths of 15 and 20 mm, respectively. The beam quality of the laser system is shown in Fig. 6(a). The beam quality was characterized [Coherent Beam Master BM-7 PCI 2968] by a BPP_{total} of 57.42 mm.mrad and 55.42 mm.mrad for the slow and fast directions, respectively. Consequently, a BPP_{total} nearly 79.8 mm.mrad was obtained.

Experiments are conducted with 600 μm and 400 μm NA0.22 optical fibers, the results in terms of coupling efficiency and emission power are shown in the Fig. 6(b). The power transmitted through the fiber was measured with a thermal pile. Maximum output power at 48 A was 45 W for 600 μm and 37 W for the 400 μm fiber. The corresponding coupling efficiencies were 87% and 75%, respectively. As it can be expected, the coupling efficiency of the 600 μm was higher than that achieved with a 40 μm fiber, since the large extent of the spot breaches the dimension of the 400 μm fiber. Furthermore, it can be seen that, in both cases, the coupling efficiency decreases with increasing injection current. This fact can be due to the decrease of the beam quality, increase of the slow-axis divergence, when increasing the injection current.[18,36] Although this effect is not drastic, it broadens the dimensions of the focus spot and thus, decreases the coupling efficiency slightly.

1. Considering all the energy losses in the system, the overall efficiency of the presented high-power diode laser optical fiber coupled system is about 57% for the 600 μm optical fibers and a 45% for the 400 μm one. Before fiber coupling, after the laser beam has passed through the dichroic beamsplitter [Fig. 2(a)], the energy losses are around 30%. This transferred energy is strongly influenced by the step-mirrors, the dichroic beamsplitter and the PBS where the relative energy lost are about 15%, 10% and 5%, respectively. The latter loss percentage fits well with the measurement of the DoP(TE) characteristic of the diode laser bar [Fig. 3(b)]. System optimization will lead to a reduction in energy losses. This optimization should be focused on improving the following aspects.
2. As described above, step-mirrors of copper, which delimit the reflectance to approximate 95% per mirror, have been used. By using dielectric mirrors, reflectivities of 99% and higher can be achieved.[37]
3. By improving the transmission energy of dichroic beamsplitter (LWP-45-RUNP633-TUNP800) at 808 nm, the current energy losses of 10% can be reduced.

On the other hand, a significant advantage of the presented laser system is its packaging cooling system. Depending on the specific requirements, different cooling techniques may be used. For high-average-power applications active cooling with water-cooled, microchannel heat sinks are necessary. For reduced average power levels, passive cooling using massive copper heat sinks mounted on thermo-electric coolers may be used.[27,38,39] In this sense, thermoelectric coolers control (TEC) have been integrated in the developed laser system [Fig. 2(b)] to remove the waste heat generated by diode laser emitters. Thus, the temperature of the junction semiconductor diode laser is held constant for injection current (optical output power).

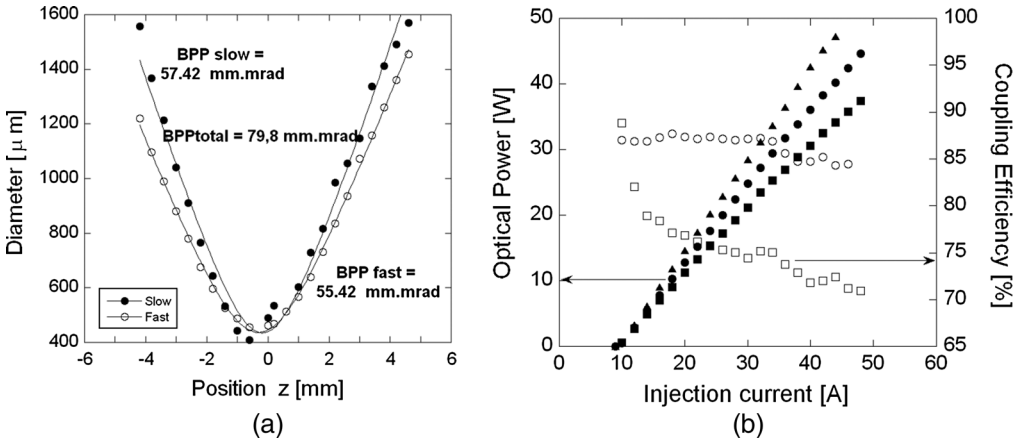

Fig. 6 (a) Beam quality measurement of the laser system at 3 W of laser power emission per bar; (b) Output power and coupling efficiency for a 600 μm and 400 μm optical fibers both with numerical aperture of 0.22 (closed triangles: input power, closed circles: output power $\Phi = 600$ μm, closed squares: Φ fiber $= 400$ μm; open circles: Φ fiber $= 600$ μm and open squares $\Phi = 400$ μm).

4 Application to Laser Transmission Welding

The diode laser system described in Secs. 2 and 3 is used for welding a wide range of thermoplastics with different physical properties. In this section, the thermoplastics and fillers considered, the experimental setup for contour laser welding and the methods used to determine the fatigue resistance of welded joints are described. Afterwards, the quality and integrity of the weld seams are analyzed in terms of the process parameters by means of an optical microscope and mechanical testing equipment, respectively.

4.1 *Materials and Methods*

In this study, the polymer employed was BASF Terluran® GP-35 ABS (ABS), a complex mixture consisting of styrene-acrylonitrile copolymer, a graft polymer of styrene-acrylonitrile and polybutadiene and some unchanged polybutadiene rubber.[40] The experimental investigation involved two types of ABS plates: the first one is a natural ABS, transparent to the infrared laser radiation, and the second one is an infrared radiation (IR)-absorbent ABS polymer (Nanocyl 700 CNTs), where carbon nanotubes (CNTs) were used as the dopant material. Contour welding experiments were performed by focusing the laser beam on the back face (partially doped ABS) and moving it over the welding contour. In this configuration, welded joints were obtained by joining two rectangular polymer sheets, partially overlapped for a length of 35 mm and a surface of 40×45 mm^2. A clamping device for flat plates, that makes a uniform pressure all around the plate contour, ensures uniform clamping pressure along the weld seam [Fig. 7(a)]. In order to analyze the influence of the doping percentage in the weld seam quality and integrity, two different weight percentages of CNTs were studied: 0.01% and 0.05%. Due to this additivation of the base polymer, both thermal and optical properties of the polymer changed significantly, affecting the final quality of the weld seam.

Micrographs of the polished cross-section of a weld were taken by using an optical microscope [Olympus SZX16 U-TV0.5xC-3]. Mechanical testing of joints was carried out by means of an universal testing machine [INStron 3369] with a maximum load capacity of 50 kN and a cross-head displacement rate of 5 mm/m in according with ASTM D638-82a "Standard Test Method for Tensile properties of plastics".

The laser beam was focused over the doped ABS plate [Fig. 7(a)] by an optical head with a 50 mm focal length. The laser beam caustic [Fig. 7(b)] was measured by means

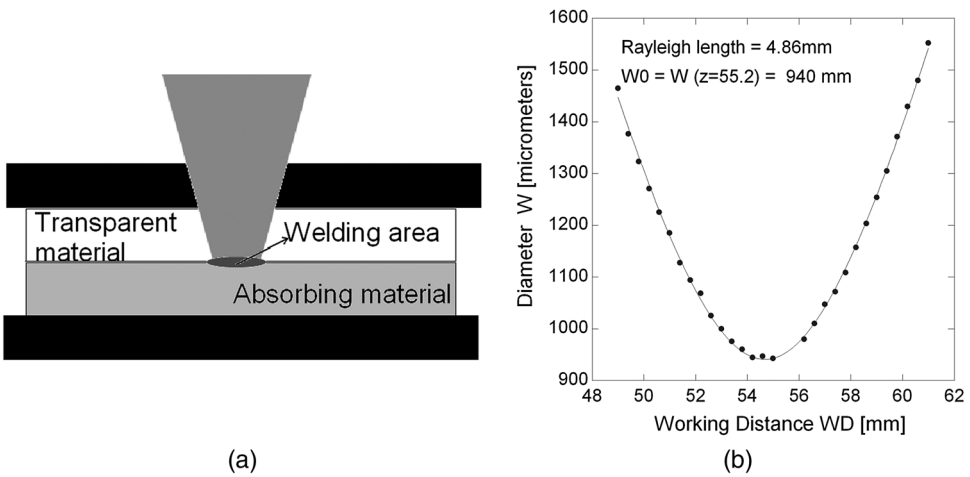

Fig. 7 (a) Schematic set-up for laser welding of two ABS plates. Bottom plate: doped ABS (CNTs) (absorbing material), top plate: natural ABS (transparent material); and (b) laser beam caustic measurement at a laser power emission of 0.5 W per bar.

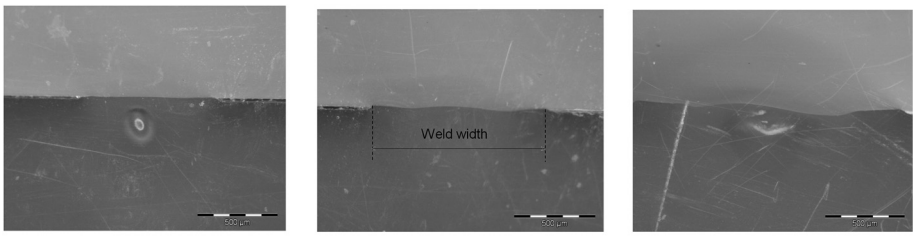

Fig. 8 Effect of the incident laser power on the weld quality: (a) poor joint: $P = 6$ W, (b) optimal joint: $P = 8.5$ W, (c) degraded joint: $P = 16.5$ W considering ABS/ABS 0.01% CNT at process speed ($v = 15$ mm/s).

of a beam analyzer [Coherent Beam Master BM 7 PCI 2968], providing a spot size (beam diameter at $1/e^2$) of $w_0 = 940 \pm 2$ μm at a working distance of 55.2 mm.

The main process parameters affecting the bond quality are: the laser power, welding speed, laser beam size and uniformity and the clamping pressure. Additionally, thermal and optical properties of the material play an important role in the welding process. LTW experiments involving natural and partially doped ABS were carried out by changing some of these key parameters: the welding speed and laser power. Thus, keeping the incident laser power constant, three different welding speeds were considered: 10, 15, and 20 mm/s, allowing us to determine the explicit relationship between laser power and welding speed, while holding all other variables constant. Contour welding experiments were performed by focusing the laser beam on the back face (partially doped ABS) and moving it over the welding contour.

4.2 *Experimental Results*

The quality and integrity of the weld seams was analyzed based on standard methods: visual inspection by optical microscopy and tensile strength analysis. As it was mentioned above, the polished cross-section of a weld was examined under a microscope. Figure 8 shows the effect of the laser power on the final weld formation and surface integrity: when the incident laser intensity is too low, a poor quality weld with pores confined in the center of the weld is obtained. When the laser intensity is too high, however, excessive heat in the joint results in material degradation. By visual inspection of the optical micrographs, high quality weld seams are characterised by a uniform melt pool profile without pores, cracks or defects [Fig. 8(b)]. In this scenario, analysis of the melt pool profile was carried out to estimate the fusion zone and, hence, the seam width.

Figure 9(a) shows the weld seam width of optimal joints as a function of the line energy (LE) for ABS with two selected percentages of CNTs. Line energy is defined as the laser power divided by the welding speed. Two regimes are observed depending on the material considered. In the case of low CNT concentration, the process window for laser welding increases significantly. It is worth to note that the overlapping area between both process windows (for high and low CNT concentration) is very small, which indicates a strong dependence of the physicochemical properties of the materials on the process parameters required for producing a defect free weld. According to the results presented in Fig. 9(a), for each CNTs concentration, the experimental data can be well fitted by a linear regression with a slope of 1284 J^{-1} and 943 J^{-1} and intercept of 312 and 717 μm for ABS−0.01% CNTs and ABS−0.05% CNTs, respectively. In the case of ABS with high CNTs concentration, some deviations are observed at low welding speeds. These results suggest that the welding process is strongly dependent on the physical (optical and thermal) properties of the material considered.

Figure 9(b) shows the average shear force prior to fracture as a function of the line energy for each welding conditions presented in Fig. 9(a). The experimental results were fitted

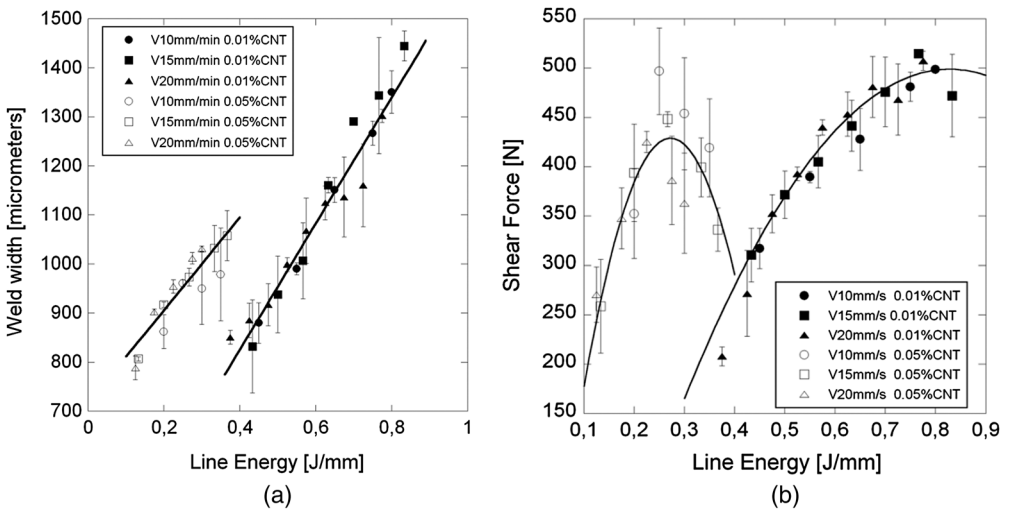

Fig. 9 Average (a) weld width (b) shear force as a function of line energy for two different percentages of CNTs.

to a second-order polynomial equation. Thus, the general trend exhibited by these experimental data is different than that observed in the case of the line energy dependence of the weld width. For ABS of low CNTs concentration, the maximum shear force occurs at about LE = 0.8 J/mm, where the weld width reaches a maximum value. This direct relationship between the shear force and the weld width was not observed for ABS containing high CNTs concentration: the shear force decreases systematically with increasing line energy when this parameter exceeds a certain threshold. According to the results presented in Fig. 9(b), this energy threshold decreases with increasing the welding speed, which may be explained in terms of the differences observe in the optical properties of the materials considered. Again, these results suggest that the sensitivity of this material to specific changes in the incident laser intensity is significantly higher than that observed in the case of ABS with low CNTs concentration.

The changing on the value of the intercept between both percentages of CNTs [Fig. 9(a)] along with the high sensitivity observed on the mechanical properties [Fig. 9(b)] suggests that the optimum processes parameters are strongly influenced by the optical properties.

5 Conclusions

A tailored diode laser system has been designed and developed for LTW application, showing a good match between modeling calculations and experimental results in terms of laser beam quality. The theoretical model has been performed using ZEMAX ray tracing software. Thus, a reliable prediction may be made for a customized laser system suitable for other industrial processes such as plastic welding. Significant advantages of the presented diode laser system are the versatility that can be achieved by means of its customization and its packaging cooling system. The latter ensures a controlled temperature of the diode laser emitters for different optical output power emission.

The developed laser system provides a beam quality of 79.8 mm.mrad, which involves coupling efficiencies of 87% and 75% for optical fibers of 600 and 400 μm, respectively. These results are in accordance with the characteristics provided by commercial diode laser systems. This set-up guarantee high quality weld seams with the required accuracy for proper packaging of miniaturized components.

The optical microscope inspections provide weld seams with good appearance and weld widths between 0.8–1.5 mm and 0.8–1.1 mm for low and high concentration of CNTs, respectively. The mechanical shear tests carried out reveal a direct relationship between shear force and weld width as function of line energy in the case of low concentration of CNTs, which is not observed for high content of fillers.

These results give rise to the assumption that the process window for ABS welding depends on the optical properties and microstructure of the material considered.

References

1. N. Amanat, N. L. James, and D. R. McKenzie, "Welding methods for joining thermoplastics polymers for the hermetic enclosure of medical device," *Med. Eng. Phys.* **32**(7), 690–699 (2010).
2. C. W. Tsao and D. L. DeVoe, "Bonding of thermoplastic polymer microfluidics," *Microfluid. Nanofluid.* **6**(1), 1–16 (2009).
3. H. Becker and C. Gartner, "Polymer microfabrication technologies for microfluidic systems," *Anal. Bioanal. Chem.* **390**(1), 89–111 (2008).
4. M. Kalpana, "Plastics welding technology for industry," *Assembly Autom.* **17**(3), 196–200 (1997).
5. T. Velten et al., "Packaging of bio–MEMS: strategies, technologies, and applications," *IEEE Trans. Adv. Packag.* **28**(4), 533–546 (2005).
6. C. Ageorges, L. Ye, and M. Hou, "Advances in fusion bonding techniques for joining thermoplastic matrix composites: a review," *Compos. Part A-Appl. Sci.* **32**(6), 839–857 (2001).
7. H. Potente, O. Karger, and G. Fiegler, "Laser and microwave welding—the applicability of new process principles," *Macromol. Mater. Eng.* **287** (11), 734–744 (2002).
8. N. C. Amanat et al., "Transmission laser welding of amorphous and semi-cristalline poly-ether-ether-ketone for applications in the medical device industry," *Mater. Design* **31**(10), 4823–4830 (2010).
9. A. M. Visco et al., "Effect of carbon nanotube amount on polyethylene welding process induced by laser source," *Appl. Phys. A-Mater.* **103**(2), 439–445 (2011).
10. J. P. Coelho, M. A. Abreu, and M. C. Pires, "High-speed laser welding of plastic films," *Opt. Lasers Eng.* **34**(4–6), 385 (2000).
11. A. Boglea, A. Olowinsky, and A. Gillner, "Fibre laser welding for packaging of disposable polymeric microfluidic–biochips," *Appl. Surf. Sci.* **254**(4), 1174–1178 (2007).
12. U. A. Russek et al., "Laser beam welding of thermoplastics," *Proc. SPIE* **4977**, 458–472 (2003).
13. J. D. Van de Ven and A. G. Erdman, "Laser transmission welding of thermoplastics- part II: experimental model validation," *J. Manuf. Sci. Eng.* **129**(5), 859–867 (2007).
14. F. Becker and H. Potente, "A step towards understanding the heating phase of laser transmission welding in polymers," *Polym. Eng. Sci.* **42**(2), 365–374 (2002).
15. E. Ghorbel, G. Casalino, and S. Abed, "Laser diode transmission welding of polypropylene: geometrical and microstructure characterization of weld," *Mater. Design* **30**(7), 2745–2751 (2009).
16. S. H. Ghasemi et al., "Beam shaping design for coupling high power diode laser stack to fiber," *Appl. Opt.* **50**(18), 2927–2930 (2011).
17. Z. Wang et al., "Fiber coupled diode laser beam parameter product calculation and rules for optimized design," *Proc. SPIE* **7918**, 791809 (2011).
18. S. Heinemann and L. Leininger, "Fiber-coupled diode lasers and beam-shaped high–power stacks," *Proc. SPIE* **3267**, 116–124 (1998).
19. P. Schreiber et al., "High-brightness fiber-coupling schemes for diode laser bars," *Proc. SPIE* **5876**, 587602 (2005).
20. H. Zbinden and J. E. Balmer, "Q-switched Nd:YLF laser end pumped by a diode-laser bar," *Opt. Lett.* **15**(18), 1014–1016 (1990).
21. T. H. Graf and J. E. Balmer, "High-power Nd:YLF laser bar end pumped by a diode-laser bar," *Opt. Lett.* **18**(16), 1317–1319 (1993).
22. S. Yamaguchi et al., "Collimation of emissions from a 1-cm aperture tightly arranged, multistripe laser-diode bar with a multiprism array coupling," *Appl. Opt.* **36**(9), 1875–1878 (1997).
23. W. A. Clarkson and D. C. Hanna, "Two-mirror beam-shaping technique for high-power diode bars," *Opt. Lett.* **21**(6), 375–377 (1996).
24. B. Ehlers et al., "Beam shaping and fiber coupling of high-power diode laser arrays," *Proc. SPIE* **3097**, 639–644 (1997).
25. R. D. Diehl, "Incoherent beam superposition and stacking," Chapter 4 in *High-Power Diode Lasers Fundamentals, Technology, Applications*, pp. 303–331, Springer (2000).
26. http://www.jenoptik.com/.
27. W. Sokolowski, D. Wolff, and P. Hennig, "Beam shaping and fiber coupling of high power diode lasers," in *Proc. Symposium on Photonics Technologies for 7th Framework Program*, pp. 129–132 (2006).
28. P. Schreiber et al., "High-brightness fiber-coupling schemes for diode laser bars," *Proc. SPIE* **5876**, 587602 (2005).
29. B. Köhler et al., "Diode laser modules base on new developments in tapered and broad area diode laser bars," *Proc. SPIE* **6876**, 68761B (2008).
30. T. Koenning et al., "Macro-channel cooled high power fiber coupled diode lasers exceeding 1.2 kW of output power," *Proc. SPIE* **7918**, 79180E (2011).
31. Z. Zuolan Wang et al., "Fiber coupled diode laser beam parameter product calculation and rules for optimized desing," *Proc. SPIE* **7918**, 791809 (2011).
32. C. Wessling et al., "50 W passively cooled, fiber coupled diode laser at 976 nm for pumping fiber lasers using 100 μm fiber bundles," *Proc. SPIE* **6876**, 687614 (2008).
33. M. Bass, "Polarization," Chapter 12 in *Handbook of Optics: Vol. I—Geometrical and Physical Optics, Polarized Light, Components and Instruments*, 3rd ed., pp. 484–488, Mc Graw Hill, New York (2010).
34. J. L. Hostetler et al., "Thermal and strain characteristics of high-power 940 nm laser arrays mounted with AuSn and In solders," *Proc. SPIE* **6456**, 645602 (2007).

35. N. Coluccelli, "Nonsequential modeling of laser diode stacks using Zemax: simulation, optimization, and experimental validation," *Appl. Opt.* **49**(22), 4237–4245 (2010).
36. B. Koehler et al., "High-brightness high-power kW system with tapered diode laser bars," *Proc. SPIE* **5711**, 73–292 (2005).
37. F. Dorsch, P. Hennig, and M. Nickel, "High-brightness fibre-couple diode laser module," *Proc. SPIE* **3285**, 192–198 (1998).
38. M. Leers and K. Boucke, "Cooling approaches for high power diode lasers," in *Conference on IEEE Electronic Components and Technology*, pp. 1011–1016, IEEE, Lake Buena Vista, FL (2008).
39. M. Leers et al., "Next generation of cooling approaches for diode laser bars," *Proc. SPIE* **6456**, 64561A (2007).
40. M. Ilie et al., "Diode laser welding of ABS: experiments and process modeling," *Opt. Laser Technol.* **41**(6), 608–614 (2009).

Eva Rodríguez-Vidal obtained her BS (September 2006) in physic and MS (February 2009) in Physics and Physical Technologies from the University of Cantabria. She joined IK4-TEKNIKER in 2007, focusing her research activity on design and development of optical systems for laser material processing applications. Nowadays, she is actively working on the study of the effect of laser radiation on the physical and chemical properties of a wide range of materials used in different industrial sector (automotive, biomedicine, energy, etc.).

Biographies and photographs of the other authors are not available.